Observation of a Charged Charmoniumlike Structure $Z_c(4020)$ and Search for the $Z_c(3900)$ in $e^+e^- \to \pi^+\pi^- h_c$

M. Ablikim,[1] M. N. Achasov,[8,*] O. Albayrak,[4] D. J. Ambrose,[41] F. F. An,[1] Q. An,[42] J. Z. Bai,[1] R. Baldini Ferroli,[19a] Y. Ban,[28] J. Becker,[3] J. V. Bennett,[18] M. Bertani,[19a] J. M. Bian,[40] E. Boger,[21,†] O. Bondarenko,[22] I. Boyko,[21] S. Braun,[37] R. A. Briere,[4] V. Bytev,[21] H. Cai,[46] X. Cai,[1] O. Cakir,[36a] A. Calcaterra,[19a] G. F. Cao,[1] S. A. Cetin,[36b] J. F. Chang,[1] G. Chelkov,[21,†] G. Chen,[1] H. S. Chen,[1] J. C. Chen,[1] M. L. Chen,[1] S. J. Chen,[26] X. R. Chen,[23] Y. B. Chen,[1] H. P. Cheng,[16] X. K. Chu,[28] Y. P. Chu,[1] D. Cronin-Hennessy,[40] H. L. Dai,[1] J. P. Dai,[1] D. Dedovich,[21] Z. Y. Deng,[1] A. Denig,[20] I. Denysenko,[21] M. Destefanis,[45a,45c] W. M. Ding,[30] Y. Ding,[24] L. Y. Dong,[1] M. Y. Dong,[1] S. X. Du,[48] J. Fang,[1] S. S. Fang,[1] L. Fava,[45b,45c] C. Q. Feng,[42] P. Friedel,[3] C. D. Fu,[1] J. L. Fu,[26] O. Fuks,[21,†] Y. Gao,[35] C. Geng,[42] K. Goetzen,[9] W. X. Gong,[1] W. Gradl,[20] M. Greco,[45a,45c] M. H. Gu,[1] Y. T. Gu,[11] Y. H. Guan,[38] A. Q. Guo,[27] L. B. Guo,[25] T. Guo,[25] Y. P. Guo,[27,20] Y. L. Han,[1] F. A. Harris,[39] K. L. He,[1] M. He,[1] Z. Y. He,[27] T. Held,[3] Y. K. Heng,[1] Z. L. Hou,[1] C. Hu,[25] H. M. Hu,[1] J. F. Hu,[37] T. Hu,[1] G. M. Huang,[5] G. S. Huang,[42] J. S. Huang,[14] L. Huang,[1] X. T. Huang,[30] Y. Huang,[26] T. Hussain,[44] C. S. Ji,[42] Q. Ji,[1] Q. P. Ji,[27] X. B. Ji,[1] X. L. Ji,[1] L. L. Jiang,[1] X. S. Jiang,[1] J. B. Jiao,[30] Z. Jiao,[16] D. P. Jin,[1] S. Jin,[1] F. F. Jing,[35] N. Kalantar-Nayestanaki,[22] M. Kavatsyuk,[22] B. Kloss,[20] B. Kopf,[3] M. Kornicer,[39] W. Kuehn,[37] W. Lai,[1] J. S. Lange,[37] M. Lara,[18] P. Larin,[13] M. Leyhe,[3] C. H. Li,[1] Cheng Li,[42] Cui Li,[42] D. L. Li,[17] D. M. Li,[48] F. Li,[1] G. Li,[1] H. B. Li,[1] J. C. Li,[1] K. Li,[12] Lei Li,[1] N. Li,[11] P. R. Li,[38] Q. J. Li,[1] W. D. Li,[1] W. G. Li,[1] X. L. Li,[30] X. N. Li,[1] X. Q. Li,[27] X. R. Li,[29] Z. B. Li,[34] H. Liang,[42] Y. F. Liang,[32] Y. T. Liang,[37] G. R. Liao,[35] D. X. Lin,[13] B. J. Liu,[1] C. L. Liu,[4] C. X. Liu,[1] F. H. Liu,[31] Fang Liu,[1] Feng Liu,[5] H. B. Liu,[11] H. H. Liu,[15] H. M. Liu,[1] J. P. Liu,[46] K. Liu,[35] K. Y. Liu,[24] P. L. Liu,[30] Q. Liu,[38] S. B. Liu,[42] X. Liu,[23] Y. B. Liu,[27] Z. A. Liu,[1] Zhiqiang Liu,[1] Zhiqing Liu,[1] H. Loehner,[22] X. C. Lou,[1,‡] G. R. Lu,[14] H. J. Lu,[16] J. G. Lu,[1] X. R. Lu,[38] Y. P. Lu,[1] C. L. Luo,[25] M. X. Luo,[47] T. Luo,[39] X. L. Luo,[1] M. Lv,[1] F. C. Ma,[24] H. L. Ma,[1] Q. M. Ma,[1] S. Ma,[1] T. Ma,[1] X. Y. Ma,[1] F. E. Maas,[13] M. Maggiora,[45a,45c] Q. A. Malik,[44] Y. J. Mao,[28] Z. P. Mao,[1] J. G. Messchendorp,[22] J. Min,[1] T. J. Min,[1] R. E. Mitchell,[18] X. H. Mo,[1] H. Moeini,[22] C. Morales Morales,[13] K. Moriya,[18] N. Yu. Muchnoi,[8,*] H. Muramatsu,[41] Y. Nefedov,[21] I. B. Nikolaev,[8,*] Z. Ning,[1] S. Nisar,[7] S. L. Olsen,[29] Q. Ouyang,[1] S. Pacetti,[19b] J. W. Park,[39] M. Pelizaeus,[3] H. P. Peng,[42] K. Peters,[9] J. L. Ping,[25] R. G. Ping,[1] R. Poling,[40] E. Prencipe,[20] M. Qi,[26] S. Qian,[1] C. F. Qiao,[38] L. Q. Qin,[30] X. S. Qin,[1] Y. Qin,[28] Z. H. Qin,[1] J. F. Qiu,[1] K. H. Rashid,[44] C. F. Redmer,[20] M. Ripka,[20] G. Rong,[1] X. D. Ruan,[11] A. Sarantsev,[21,§] S. Schumann,[20] W. Shan,[28] M. Shao,[42] C. P. Shen,[2] X. Y. Shen,[1] H. Y. Sheng,[1] M. R. Shepherd,[18] W. M. Song,[1] X. Y. Song,[1] S. Spataro,[45a,45c] B. Spruck,[37] G. X. Sun,[1] J. F. Sun,[14] S. S. Sun,[1] Y. J. Sun,[42] Y. Z. Sun,[1] Z. J. Sun,[1] Z. T. Sun,[42] C. J. Tang,[32] X. Tang,[1] I. Tapan,[36c] E. H. Thorndike,[41] D. Toth,[40] M. Ullrich,[37] I. Uman,[36b] G. S. Varner,[39] B. Wang,[1] D. Wang,[28] D. Y. Wang,[28] K. Wang,[1] L. L. Wang,[1] L. S. Wang,[1] M. Wang,[30] P. Wang,[1] P. L. Wang,[1] Q. J. Wang,[1] S. G. Wang,[28] X. F. Wang,[35] X. L. Wang,[42] Y. D. Wang,[19a] Y. F. Wang,[1] Y. Q. Wang,[20] Z. Wang,[1] Z. G. Wang,[1] Z. H. Wang,[42] Z. Y. Wang,[1] D. H. Wei,[10] J. B. Wei,[28] P. Weidenkaff,[20] Q. G. Wen,[42] S. P. Wen,[1] M. Werner,[37] U. Wiedner,[3] L. H. Wu,[1] N. Wu,[1] S. X. Wu,[42] W. Wu,[27] Z. Wu,[1] L. G. Xia,[35] Y. X. Xia,[17] Z. J. Xiao,[25] Y. G. Xie,[1] Q. L. Xiu,[1] G. F. Xu,[1] Q. J. Xu,[12] Q. N. Xu,[38] X. P. Xu,[33] Z. R. Xu,[42] Z. Xue,[1] L. Yan,[42] W. B. Yan,[42] W. C. Yan,[42] Y. H. Yan,[17] H. X. Yang,[1] Y. Yang,[5] Y. X. Yang,[10] Y. Z. Yang,[11] H. Ye,[1] M. Ye,[1] M. H. Ye,[6] B. X. Yu,[1] C. X. Yu,[27] H. W. Yu,[28] J. S. Yu,[23] S. P. Yu,[30] C. Z. Yuan,[1] W. L. Yuan,[26] Y. Yuan,[1] A. A. Zafar,[44] A. Zallo,[19a] S. L. Zang,[26] Y. Zeng,[17] B. X. Zhang,[1] B. Y. Zhang,[1] C. Zhang,[26] C. B. Zhang,[17] C. C. Zhang,[1] D. H. Zhang,[1] H. H. Zhang,[34] H. Y. Zhang,[1] J. Q. Zhang,[1] J. W. Zhang,[1] J. Y. Zhang,[1] J. Z. Zhang,[1] LiLi Zhang,[17] S. H. Zhang,[1] X. J. Zhang,[1] X. Y. Zhang,[30] Y. Zhang,[1] Y. H. Zhang,[1] Z. P. Zhang,[42] Z. Y. Zhang,[46] Zhenghao Zhang,[5] G. Zhao,[1] J. W. Zhao,[1] Lei Zhao,[42] Ling Zhao,[1] M. G. Zhao,[27] Q. Zhao,[1] S. J. Zhao,[48] T. C. Zhao,[1] X. H. Zhao,[26] Y. B. Zhao,[1] Z. G. Zhao,[42] A. Zhemchugov,[21,†] B. Zheng,[43] J. P. Zheng,[1] Y. H. Zheng,[38] B. Zhong,[25] L. Zhou,[1] X. Zhou,[46] X. K. Zhou,[38] X. R. Zhou,[42] K. Zhu,[1] K. J. Zhu,[1] X. L. Zhu,[35] Y. C. Zhu,[42] Y. S. Zhu,[1] Z. A. Zhu,[1] J. Zhuang,[1] B. S. Zou,[1] and J. H. Zou[1]

(BESIII Collaboration)

[1]*Institute of High Energy Physics, Beijing 100049, People's Republic of China*
[2]*Beihang University, Beijing 100191, People's Republic of China*
[3]*Bochum Ruhr-University, D-44780 Bochum, Germany*
[4]*Carnegie Mellon University, Pittsburgh, Pennsylvania 15213, USA*

[5]Central China Normal University, Wuhan 430079, People's Republic of China
[6]China Center of Advanced Science and Technology, Beijing 100190, People's Republic of China
[7]COMSATS Institute of Information Technology, Lahore, Defence Road, Off Raiwind Road, 54000 Lahore, Pakistan
[8]G. I. Budker Institute of Nuclear Physics SB RAS (BINP), Novosibirsk 630090, Russia
[9]GSI Helmholtzcentre for Heavy Ion Research GmbH, D-64291 Darmstadt, Germany
[10]Guangxi Normal University, Guilin 541004, People's Republic of China
[11]GuangXi University, Nanning 530004, People's Republic of China
[12]Hangzhou Normal University, Hangzhou 310036, People's Republic of China
[13]Helmholtz Institute Mainz, Johann-Joachim-Becher-Weg 45, D-55099 Mainz, Germany
[14]Henan Normal University, Xinxiang 453007, People's Republic of China
[15]Henan University of Science and Technology, Luoyang 471003, People's Republic of China
[16]Huangshan College, Huangshan 245000, People's Republic of China
[17]Hunan University, Changsha 410082, People's Republic of China
[18]Indiana University, Bloomington, Indiana 47405, USA
[19a]INFN Laboratori Nazionali di Frascati, I-00044, Frascati, Italy
[19b]INFN and University of Perugia, I-06100, Perugia, Italy
[20]Johannes Gutenberg University of Mainz, Johann-Joachim-Becher-Weg 45, D-55099 Mainz, Germany
[21]Joint Institute for Nuclear Research, 141980 Dubna, Moscow region, Russia
[22]KVI, University of Groningen, NL-9747 AA Groningen, Netherlands
[23]Lanzhou University, Lanzhou 730000, People's Republic of China
[24]Liaoning University, Shenyang 110036, People's Republic of China
[25]Nanjing Normal University, Nanjing 210023, People's Republic of China
[26]Nanjing University, Nanjing 210093, People's Republic of China
[27]Nankai University, Tianjin 300071, People's Republic of China
[28]Peking University, Beijing 100871, People's Republic of China
[29]Seoul National University, Seoul, 151-747 Korea
[30]Shandong University, Jinan 250100, People's Republic of China
[31]Shanxi University, Taiyuan 030006, People's Republic of China
[32]Sichuan University, Chengdu 610064, People's Republic of China
[33]Soochow University, Suzhou 215006, People's Republic of China
[34]Sun Yat-Sen University, Guangzhou 510275, People's Republic of China
[35]Tsinghua University, Beijing 100084, People's Republic of China
[36a]Ankara University, Dogol Caddesi, 06100 Tandogan, Ankara, Turkey
[36b]Dogus University, 34722 Istanbul, Turkey
[36c]Uludag University, 16059 Bursa, Turkey
[37]Universitaet Giessen, D-35392 Giessen, Germany
[38]University of Chinese Academy of Sciences, Beijing 100049, People's Republic of China
[39]University of Hawaii, Honolulu, Hawaii 96822, USA
[40]University of Minnesota, Minneapolis, Minnesota 55455, USA
[41]University of Rochester, Rochester, New York 14627, USA
[42]University of Science and Technology of China, Hefei 230026, People's Republic of China
[43]University of South China, Hengyang 421001, People's Republic of China
[44]University of the Punjab, Lahore-54590, Pakistan
[45a]University of Turin, I-10125, Turin, Italy
[45b]University of Eastern Piedmont, I-15121 Alessandria, Italy
[45c]INFN, I-10125, Turin, Italy
[46]Wuhan University, Wuhan 430072, People's Republic of China
[47]Zhejiang University, Hangzhou 310027, People's Republic of China
[48]Zhengzhou University, Zhengzhou 450001, People's Republic of China
(Received 7 September 2013; published 10 December 2013)

We study $e^+e^- \to \pi^+\pi^- h_c$ at center-of-mass energies from 3.90 to 4.42 GeV by using data samples collected with the BESIII detector operating at the Beijing Electron Positron Collider. The Born cross sections are measured at 13 energies and are found to be of the same order of magnitude as those of $e^+e^- \to \pi^+\pi^- J/\psi$ but with a different line shape. In the $\pi^\pm h_c$ mass spectrum, a distinct structure, referred to as $Z_c(4020)$, is observed at 4.02 GeV/c^2. The $Z_c(4020)$ carries an electric charge and couples to charmonium. A fit to the $\pi^\pm h_c$ invariant mass spectrum, neglecting possible interferences, results in a mass of $(4022.9 \pm 0.8 \pm 2.7)$ MeV/c^2 and a width of $(7.9 \pm 2.7 \pm 2.6)$ MeV for the $Z_c(4020)$, where the first errors are statistical and the second systematic. The difference between the parameters of this structure and the $Z_c(4025)$ observed in the $D^*\bar{D}^*$ final state is within 1.5σ, but

whether they are the same state needs further investigation. No significant $Z_c(3900)$ signal is observed, and upper limits on the $Z_c(3900)$ production cross sections in $\pi^{\pm}h_c$ at center-of-mass energies of 4.23 and 4.26 GeV are set.

DOI: 10.1103/PhysRevLett.111.242001 PACS numbers: 14.40.Rt, 13.66.Bc, 14.40.Pq

In the study of the $e^+e^- \to \pi^+\pi^- J/\psi$ at center-of-mass (c.m.) energies around 4.26 GeV, the BESIII [1] and Belle [2] experiments observed a charged charmoniumlike state, the $Z_c(3900)$, which was confirmed shortly after with CLEO data at a c.m. energy of 4.17 GeV [3]. As there are at least four quarks within the $Z_c(3900)$, it is interpreted as either a tetraquark state, a $D\bar{D}^*$ molecule, hadroquarkonium, or other configurations [4]. More recently, BESIII has observed another charged $Z_c(4025)$ state in $e^+e^- \to \pi^{\pm}(D^*\bar{D}^*)^{\mp}$ [5]. These states together with similar states observed in the bottomonium system [6] would seem to indicate that a new class of hadrons has been observed.

Such a particle may couple to $\pi^{\pm}h_c$ [4] and thus can be searched for in $e^+e^- \to \pi^+\pi^- h_c$. This final state has been studied by CLEO [7], and a hint of a rising cross section at 4.26 GeV has been observed. An improved measurement may shed light on understanding the nature of the $Y(4260)$ as well [8,9].

In this Letter, we present a study of $e^+e^- \to \pi^+\pi^- h_c$ at 13 c.m. energies from 3.900 to 4.420 GeV. The data samples were collected with the BESIII detector [10] and are listed in Table I. The c.m. energies ($\sqrt{s}$) are measured with a beam energy measurement system [12] with an uncertainty of ± 1.0 MeV. A charged structure is observed in the $\pi^{\pm}h_c$ invariant mass spectrum at 4.02 GeV/c^2 [referred to as the $Z_c(4020)$ hereafter]. We also report on the search for $Z_c(3900)$ decays into the same final state. No significant signal is observed, and an upper limit on the production rate is determined. In the studies presented here, the h_c is reconstructed via its electric-dipole ($E1$) transition $h_c \to \gamma\eta_c$ with $\eta_c \to X_i$, where X_i signifies 16 exclusive hadronic final states: $p\bar{p}$, $2(\pi^+\pi^-)$, $2(K^+K^-)$, $K^+K^-\pi^+\pi^-$, $p\bar{p}\pi^+\pi^-$, $3(\pi^+\pi^-)$, $K^+K^-2(\pi^+\pi^-)$, $K^0_SK^{\pm}\pi^{\mp}$, $K^0_SK^{\pm}\pi^{\mp}\pi^{\pm}\pi^{\mp}$, $K^+K^-\pi^0$, $p\bar{p}\pi^0$, $\pi^+\pi^-\eta$, $K^+K^-\eta$, $2(\pi^+\pi^-)\eta$, $\pi^+\pi^-\pi^0\pi^0$, and $2(\pi^+\pi^-)\pi^0\pi^0$.

TABLE I. $e^+e^- \to \pi^+\pi^- h_c$ cross sections (or upper limits at the 90% confidence level). The third errors are from the uncertainty in $\mathcal{B}(h_c \to \gamma\eta_c)$ [11].

$\sqrt{s}$ (GeV)	$\mathcal{L}$ (pb^{-1})	$n^{\rm obs}_{h_c}$	$\sigma(e^+e^- \to \pi^+\pi^- h_c)$ (pb)
3.900	52.8	<2.3	<8.3
4.009	482.0	<13	<5.0
4.090	51.0	<6.0	<13
4.190	43.0	8.8 ± 4.9	$17.7 \pm 9.8 \pm 1.6 \pm 2.8$
4.210	54.7	21.7 ± 5.9	$34.8 \pm 9.5 \pm 3.2 \pm 5.5$
4.220	54.6	26.6 ± 6.8	$41.9 \pm 10.7 \pm 3.8 \pm 6.6$
4.230	1090.0	646 ± 33	$50.2 \pm 2.7 \pm 4.6 \pm 7.9$
4.245	56.0	22.6 ± 7.1	$32.7 \pm 10.3 \pm 3.0 \pm 5.1$
4.260	826.8	416 ± 28	$41.0 \pm 2.8 \pm 3.7 \pm 6.4$
4.310	44.9	34.6 ± 7.2	$61.9 \pm 12.9 \pm 5.6 \pm 9.7$
4.360	544.5	357 ± 25	$52.3 \pm 3.7 \pm 4.8 \pm 8.2$
4.390	55.1	30.0 ± 7.8	$41.8 \pm 10.8 \pm 3.8 \pm 6.6$
4.420	44.7	29.1 ± 7.3	$49.4 \pm 12.4 \pm 4.5 \pm 7.6$

We select charged tracks, photons, and $K^0_S \to \pi^+\pi^-$ candidates as described in Ref. [13]. A candidate π^0 (η) is reconstructed from pairs of photons with an invariant mass in the range $|M_{\gamma\gamma} - m_{\pi^0}| < 15$ MeV/c^2 ($|M_{\gamma\gamma} - m_{\eta}| < 15$ MeV/c^2), where m_{π^0} (m_{η}) is the nominal π^0 (η) mass [14].

In selecting $e^+e^- \to \pi^+\pi^- h_c$, $h_c \to \gamma\eta_c$ candidates, all charged tracks are assumed to be pions, and events with at least one combination satisfying $M^{\rm recoil}_{\pi^+\pi^-} \in [3.45, 3.65]$ GeV/c^2 and $M^{\rm recoil}_{\gamma\pi^+\pi^-} \in [2.8, 3.2]$ GeV/c^2 are kept for further analysis. Here $M^{\rm recoil}_{\pi^+\pi^-}$ ($M^{\rm recoil}_{\gamma\pi^+\pi^-}$) is the mass recoiling from the $\pi^+\pi^-$ ($\gamma\pi^+\pi^-$) pair, which should be in the mass range of the h_c (η_c).

To determine the species of final state particles and to select the best photon when additional photons (and π^0 or η candidates) are found in an event, the combination with the minimum value of $\chi^2 = \chi^2_{\rm 4C} + \sum_{i=1}^{N}\chi^2_{\rm PID}(i) + \chi^2_{\rm 1C}$ is selected for further analysis, where $\chi^2_{\rm 4C}$ is the χ^2 from the initial-final four-momentum conservation (4C) kinematic fit and $\chi^2_{\rm PID}(i)$ is the χ^2 from particle identification (PID) using the energy loss in the main draft chamber and the time measured with the time-of-flight system. N is the number of the charged tracks in the final states, and $\chi^2_{\rm 1C}$ is the sum of the 1C (mass constraint of the two daughter photons) χ^2 of the π^0 and η in each final state. There is also a $\chi^2_{\rm 4C}$ requirement, which is optimized by using the figure of merit $S/\sqrt{S+B}$, where S and B are the numbers of Monte Carlo (MC) simulated signal and background events, respectively, and $\chi^2_{\rm 4C} < 35$ (efficiency is about 80% from MC simulation) is required for final states with only charged or K^0_S particles, while $\chi^2_{\rm 4C} < 20$ (efficiency is about 70% from MC simulation) is required for those with π^0 or η [15]. A similar optimization procedure determines the η_c candidate mass window around the nominal η_c [14] mass to be ± 50 MeV/c^2 with efficiency about 85% from MC simulation (± 45 MeV/c^2 with efficiency about 80% from MC simulation) for final states with only charged or K^0_S particles (those with π^0 or η).

Figure 1 shows as an example the scatter plot of the mass of the η_c candidate versus that of the h_c candidate at the c.m. energy of 4.26 GeV, as well as the projection of the invariant mass distribution of $\gamma\eta_c$ in the η_c signal region,

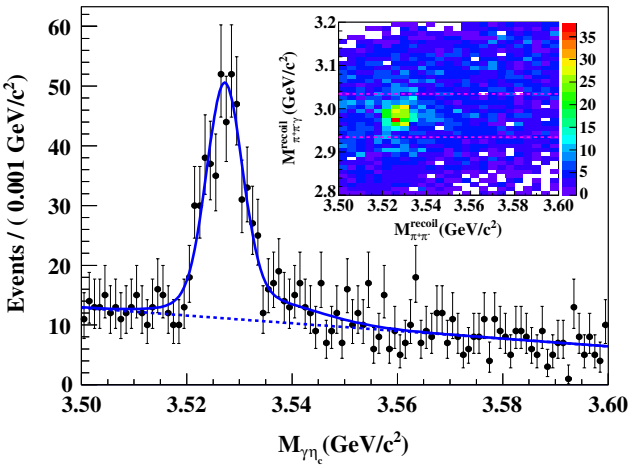

FIG. 1 (color online). The $M_{\gamma\eta_c}$ distribution after the η_c signal selection of 4.26 GeV data: dots with error bars are data, and the curves are the best fit described in the text. The inset is the scatter plot of the mass of the η_c candidate versus that of the h_c candidate.

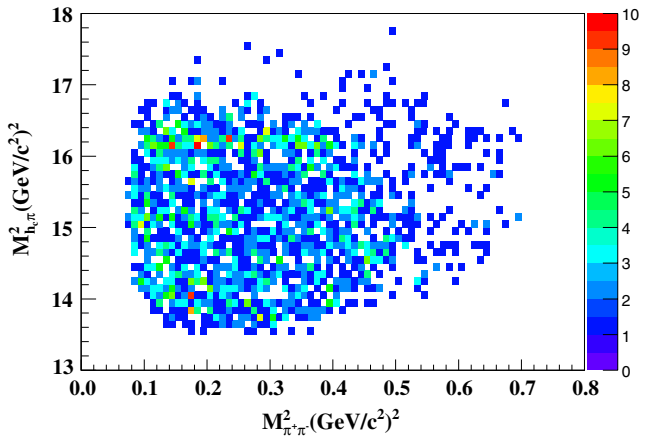

FIG. 2 (color online). Dalitz plot ($M^2_{\pi^+ h_c}$ vs $M^2_{\pi^+\pi^-}$) for selected $e^+e^- \to \pi^+\pi^- h_c$ events, summed over all energy points.

where a clear $h_c \to \gamma\eta_c$ signal is observed. To extract the number of $\pi^+\pi^- h_c$ signal events, the $\gamma\eta_c$ mass spectrum is fitted by using the MC simulated signal shape convolved with a Gaussian function to reflect the mass resolution difference (around 10%) between the data and MC simulation, together with a linear background. The fit to the 4.26 GeV data is shown in Fig. 1. The tail in the high mass side is due to the events with initial state radiation (ISR), which is simulated well in MC, and its fraction is fixed in the fit. At the energy points with large statistics (4.23, 4.26, and 4.36 GeV), the fit is applied to the 16 η_c decay modes simultaneously, while, at the other energy points, we fit the mass spectrum summed over all the η_c decay modes. The number of signal events ($n^{\rm obs}_{h_c}$) and the measured Born cross section at each energy are listed in Table I. The $\pi^+\pi^- h_c$ cross section appears to be constant above 4.2 GeV with a possible local maximum at around 4.23 GeV. This is in contrast to the observed energy dependence in the $e^+e^- \to \pi^+\pi^- J/\psi$ channel which revealed a decrease of cross sections at higher energies [2,17].

Systematic errors in the cross section measurement mainly come from the luminosity measurement, the branching fraction of $h_c \to \gamma\eta_c$, the branching fraction of $\eta_c \to X_i$, the detection efficiency, the ISR correction factor, and the fit. The integrated luminosity at each energy point is measured by using large angle Bhabha events, and it has an estimated uncertainty of 1.2%. The branching fractions of $h_c \to \gamma\eta_c$ and $\eta_c \to X_i$ are taken from Refs. [11,13]. The uncertainties in the detection efficiency are estimated in the same way as described in Refs. [13,16], and the error in the ISR correction is estimated as described in Ref. [1]. Uncertainties due to the choice of the signal shape, the background shape, the mass resolution, and the fit range are estimated by varying the h_c and η_c resonant parameters and line shapes in the MC simulation, varying the background function from linear to a second-order polynomial, varying the mass resolution difference between data and MC simulation by one standard deviation, and by extending the fit range. Assuming all of the sources are independent, the total systematic error in the $\pi^+\pi^- h_c$ cross section measurement is determined to be between 7% and 9% depending on the energy, and to be conservative we take 9% for all the energy points. The uncertainty in $\mathcal{B}(h_c \to \gamma\eta_c)$ is 15.7% [14], common to all energy points, and quoted separately in the cross section measurement. Altogether, about 95% of the total systematic errors are common to all the energy points.

Intermediate states are studied by examining the Dalitz plot of the selected $\pi^+\pi^- h_c$ candidate events. The h_c signal is selected by using $3.518 < M_{\gamma\eta_c} < 3.538$ GeV/c^2 and the sideband by using $3.490 < M_{\gamma\eta_c} < 3.510$ GeV/c^2 or $3.560 < M_{\gamma\eta_c} < 3.580$ GeV/c^2, which is twice as wide as the signal region. Figure 2 shows the Dalitz plot of the $\pi^+\pi^- h_c$ candidate events summed over all energies. While there are no clear structures in the $\pi^+\pi^-$ system, there is clear evidence for an exotic charmoniumlike structure in the $\pi^\pm h_c$ system. Figure 3 shows the projection of the $M_{\pi^\pm h_c}$ (two entries per event) distribution for the signal events, as well as the background events estimated from normalized h_c mass sidebands. There is a significant peak at around 4.02 GeV/c^2 [the $Z_c(4020)$], and the wider peak at low masses is the reflection of the $Z_c(4020)$. There are also some events at around 3.9 GeV/c^2, which could be the $Z_c(3900)$. The individual data sets at 4.23, 4.26, and 4.36 GeV show similar structures.

An unbinned maximum likelihood fit is applied to the $M_{\pi^\pm h_c}$ distribution summed over the 16 η_c decay modes. The data at 4.23, 4.26, and 4.36 GeV are fitted simultaneously with the same signal function with common mass and width. The signal shape is parametrized as a constant width relativistic Breit-Wigner function convolved with a

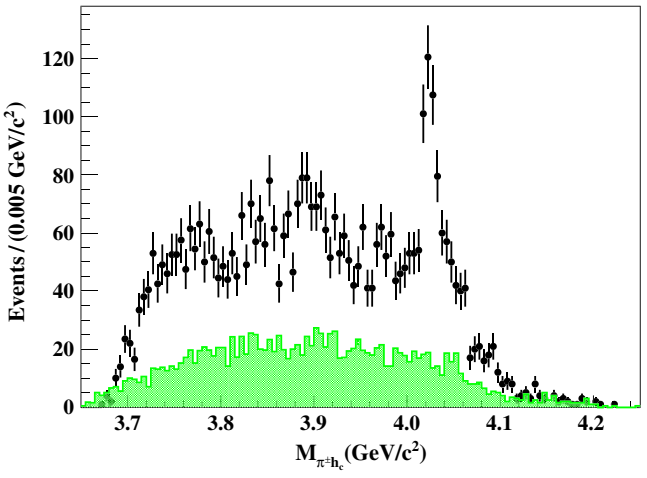

FIG. 3 (color online). $M_{\pi^\pm h_c}$ distribution of $e^+e^- \to \pi^+\pi^- h_c$ candidate events in the h_c signal region (dots with error bars) and the normalized h_c sideband region (shaded histogram), summed over data at all energy points.

Gaussian with a mass resolution determined from the data directly. Assuming the spin parity of the $Z_c(4020)$ $J^P = 1^+$, a phase space factor pq^3 is considered in the partial width, where p is the $Z_c(4020)$ momentum in the e^+e^- c.m. frame and q is the h_c momentum in the $Z_c(4020)$ c.m. frame. The background shape is parametrized as an ARGUS function [18]. The efficiency curve is considered in the fit, but possible interferences between the signal and background are neglected. Figure 4 shows the fit results; the fit yields a mass of (4022.9 ± 0.8) MeV/c^2 and a width of (7.9 ± 2.7) MeV. The goodness of fit is found to be $\chi^2/\text{n.d.f.} = 27.3/32 = 0.85$ by projecting the events into

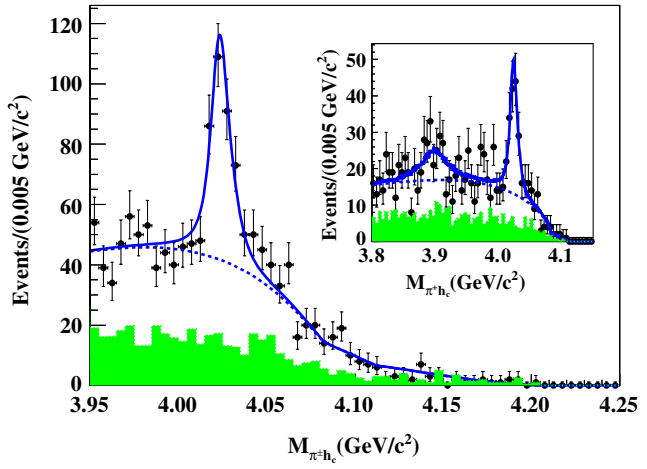

FIG. 4 (color online). Sum of the simultaneous fits to the $M_{\pi^\pm h_c}$ distributions at 4.23, 4.26, and 4.36 GeV as described in the text; the inset shows the sum of the simultaneous fit to the $M_{\pi^+ h_c}$ distributions at 4.23 and 4.26 GeV with $Z_c(3900)$ and $Z_c(4020)$. Dots with error bars are data; shaded histograms are the normalized sideband background; the solid curves show the total fit, and the dotted curves the backgrounds from the fit.

a histogram with 46 bins. The statistical significance of the $Z_c(4020)$ signal is calculated by comparing the fit likelihoods with and without the signal. Besides the nominal fit, the fit is also performed by changing the fit range, the signal shape, or the background shape. In all cases, the significance is found to be greater than 8.9σ.

The numbers of $Z_c(4020)$ events are determined to be $N[Z_c(4020)^\pm] = 114 \pm 25$, 72 ± 17, and 67 ± 15 at 4.23, 4.26, and 4.36 GeV, respectively. The cross sections are calculated to be $\sigma[e^+e^- \to \pi^\pm Z_c(4020)^\mp \to \pi^+\pi^- h_c] = (8.7 \pm 1.9 \pm 2.8 \pm 1.4)$ pb at 4.23 GeV, $(7.4 \pm 1.7 \pm 2.1 \pm 1.2)$ pb at 4.26 GeV, and $(10.3 \pm 2.3 \pm 3.1 \pm 1.6)$ pb at 4.36 GeV, where the first errors are statistical, the second ones systematic (described in detail below), and the third ones from the uncertainty in $\mathcal{B}(h_c \to \gamma\eta_c)$ [14]. The $Z_c(4020)$ production rate is uniform at these three energy points.

Adding a $Z_c(3900)$ with the mass and width fixed to the BESIII measurement [1] in the fit results in a statistical significance of 2.1σ (see the inset in Fig. 4). We set upper limits on the production cross sections as $\sigma[e^+e^- \to \pi^\pm Z_c(3900)^\mp \to \pi^+\pi^- h_c] < 13$ pb at 4.23 GeV and <11 pb at 4.26 GeV, at the 90% confidence level (C.L.). The probability density function from the fit is smeared by a Gaussian function with a standard deviation of σ_{sys} to include the systematic error effect, where σ_{sys} is the relative systematic error in the cross section measurement described below. We do not fit the 4.36 GeV data, as the $Z_c(3900)$ signal overlaps with the reflection of the $Z_c(4020)$ signal.

The systematic errors for the resonance parameters of the $Z_c(4020)$ come from the mass calibration, parametrization of the signal and background shapes, possible existence of the $Z_c(3900)$ and interference with it, fitting range, efficiency curve, and mass resolution. The uncertainty from the mass calibration is estimated by using the difference between the measured and known h_c masses and D^0 masses (reconstructed from $K^-\pi^+$). The differences are (2.1 ± 0.4) and $-(0.7 \pm 0.2)$ MeV/c^2, respectively. Since our signal topology has one low momentum pion and many tracks from the h_c decay, we assume these differences added in quadrature, 2.6 MeV/c^2, is the systematic error due to the mass calibration. Spin parity conservation forbids a zero spin for the $Z_c(4020)$, and, assuming that contributions from D wave or higher are negligible, the only alternative is $J^P = 1^-$ for the $Z_c(4020)$. A fit under this scenario yields a mass difference of 0.2 MeV/c^2 and a width difference of 0.8 MeV. The uncertainty due to the background shape is determined by changing to a second-order polynomial and by varying the fit range. A difference of 0.1 MeV/c^2 for the mass is found from the former, and differences of 0.2 MeV/c^2 for mass and 1.1 MeV for width are found from the latter. Uncertainties due to the mass resolution are estimated by varying the resolution difference between the data and MC simulation by one standard

TABLE II. The percentage systematic errors in $\sigma[e^+e^- \to \pi^\pm Z_c(4020)^\mp \to \pi^+\pi^- h_c]$, in addition to those in the $\sigma(e^+e^- \to \pi^+\pi^- h_c)$ measurement.

$\sqrt{s}$ (GeV)	$Z_c(3900)$ signal	Interference	Fitting range	Signal shape	Background shape	h_c signal window	Mass resolution	Efficiency curve
4.230	18.3	20.0	13.2	4.5	3.5	1.7	1.8	0.9
4.260	16.2	20.0	8.3	4.2	2.8	1.7	1.8	0.0
4.360	18.3	20.0	4.5	6.0	6.0	1.4	1.5	0.0

deviation of the measured uncertainty in the mass resolution of the h_c signal; the difference is 0.5 MeV in the width, which is taken as the systematic error. The uncertainty in the efficiency curve results in 0.1 MeV/c^2 for mass and 0.1 MeV for width. Uncertainties due to the possible existence of the $Z_c(3900)$ and the interference with it are estimated by adding a $Z_c(3900)$ amplitude incoherently or coherently in the fit. The uncertainties due to $Z_c(3900)$ are 0.2 MeV/c^2 for mass and 2.1 MeV for width, while the uncertainties due to interference are 0.5 MeV/c^2 for the mass and 0.4 MeV for the width. Assuming all the sources of systematic uncertainty are independent, the total systematic error is 2.7 MeV/c^2 for the mass and 2.6 MeV for the width.

The systematic errors in $\sigma[e^+e^- \to \pi^\pm Z_c(4020)^\mp \to \pi^+\pi^- h_c]$ are estimated in the same way as for $\sigma(e^+e^- \to \pi^+\pi^- h_c)$. The systematic errors due to the inclusion of the $Z_c(3900)$ signal, the possible interference between $Z_c(4020)$ and $Z_c(3900)$, the fitting range, the signal and background parametrizations, the h_c signal window selection, the mass resolution, and the efficiency curve, in addition to those in the $\sigma(e^+e^- \to \pi^+\pi^- h_c)$ measurement, are considered and summarized in Table II. The systematic errors in $\sigma[e^+e^- \to \pi^\pm Z_c(3900)^\mp \to \pi^+\pi^- h_c]$ are determined similarly.

In summary, we measure $e^+e^- \to \pi^+\pi^- h_c$ cross sections at c.m. energies between 3.90 and 4.42 GeV for the first time. These cross sections are of the same order of magnitude as those of the $e^+e^- \to \pi^+\pi^- J/\psi$ measured by BESIII [1] and other experiments [2,17] but with a different line shape. There is a broad structure at high energy with a possible local maximum at around 4.23 GeV. A narrow structure very close to the $(D^*\bar{D}^*)^\pm$ threshold with a mass of $(4022.9 \pm 0.8 \pm 2.7)$ MeV/c^2 and a width of $(7.9 \pm 2.7 \pm 2.6)$ MeV is observed in the $\pi^\pm h_c$ mass spectrum. This structure couples to charmonium and has an electric charge, which is suggestive of a state containing more quarks than just a charm and an anticharm quark, as the $Z_c(3900)$ observed in the $\pi^\pm J/\psi$ system [1–3]. We do not find a significant signal for $Z_c(3900) \to \pi^\pm h_c$, and the production cross section is found to be smaller than 11 pb at the 90% C.L. at 4.26 GeV, which is lower than that of $Z_c(3900) \to \pi^\pm J/\psi$ [1]. The $Z_c(4020)$ parameters agree within 1.5σ of those of the $Z_c(4025)$, observed in $e^+e^- \to \pi^\pm(D^*\bar{D}^*)^\mp$ at a c.m. energy 4.26 GeV [5]. Results for the latter at 4.23 and 4.36 GeV may help us to understand whether they are the same state.

The BESIII Collaboration thanks the staff of BEPCII and the computing center for their strong support. This work is supported in part by the Ministry of Science and Technology of China under Contract No. 2009CB825200; National Natural Science Foundation of China (NSFC) under Contracts No. 10625524, No. 10821063, No. 10825524, No. 10835001, No. 10935007, No. 11125525, and No. 11235011; Joint Funds of the National Natural Science Foundation of China under Contracts No. 11079008, No. 11079023, No. 11179007, and No. U1332201; the Chinese Academy of Sciences (CAS) Large-Scale Scientific Facility Program; CAS under Contracts No. KJCX2-YW-N29 and No. KJCX2-YW-N45; 100 Talents Program of CAS; German Research Foundation DFG under Collaborative Research Center Contract No. CRC-1044; Istituto Nazionale di Fisica Nucleare, Italy; Ministry of Development of Turkey under Contract No. DPT2006K-120470; U.S. Department of Energy under Contracts No. DE-FG02-04ER41291, No. DE-FG02-05ER41374, and No. DE-FG02-94ER40823; U.S. National Science Foundation; University of Groningen (RuG) and the Helmholtzzentrum fuer Schwerionenforschung GmbH (GSI), Darmstadt; WCU Program of National Research Foundation of Korea under Contract No. R32-2008-000-10155-0.

*Also at the Novosibirsk State University, Novosibirsk, 630090, Russia.
†Also at the Moscow Institute of Physics and Technology, Moscow 141700, Russia.
‡Also at University of Texas at Dallas, Richardson, TX 75083, USA.
§Also at the PNPI, Gatchina 188300, Russia.

[1] M. Ablikim *et al.* (BESIII Collaboration), Phys. Rev. Lett. **110**, 252001 (2013).
[2] Z. Q. Liu *et al.* (Belle Collaboration), Phys. Rev. Lett. **110**, 252002 (2013).
[3] T. Xiao, S. Dobbs, A. Tomaradze, and K. K. Seth, arXiv:1304.3036.
[4] Q. Wang, C. Hanhart, and Q. Zhao, Phys. Rev. Lett. **111**, 132003 (2013); F.-K. Guo, C. Hidalgo-Duque, J. Nieves, and M. P. Valderrama, Phys. Rev. D **88**, 054007 (2013); G. Li, arXiv:1304.4458 [Eur. Phys. J. C (to be published)];

C.-Y. Cui, Y.-L. Liu, W.-B. Chen, and M.-Q. Huang, arXiv:1304.1850; J.-R. Zhang, Phys. Rev. D **87**, 116004 (2013); J. M. Dias, F. S. Navarra, M. Nielsen, and C. M. Zanetti, Phys. Rev. D **88**, 016004 (2013); M. B. Voloshin, Phys. Rev. D **87**, 091501 (2013); E. Braaten, Phys. Rev. Lett. **111**, 162003 (2013); E. Wilbring, H. W. Hammer, and U. G. Meißner, Phys. Lett. B **726**, 326 (2013); D.-Y. Chen, X. Liu, and T. Matsuki, Phys. Rev. D **88**, 036008 (2013); K. Terasaki, arXiv:1304.7080; Y.-R. Liu, Phys. Rev. D **88**, 074008 (2013); Q. Wang, C. Hanhart, and Q. Zhao, Phys. Lett. B **725**, 106 (2013); Y. Dong, A. Faessler, T. Gutsche, and V. E. Lyubovitskij, Phys. Rev. D **88**, 014030 (2013); X.-H. Liu and G. Li, Phys. Rev. D **88**, 014013 (2013); S. Prelovsek and L. Leskovec, arXiv:1308.2097 [Phys. Lett. B (to be published)].

[5] M. Ablikim *et al.* (BESIII Collaboration), arXiv:1308.2760.

[6] A. Bondar *et al.* (Belle Collaboration), Phys. Rev. Lett. **108**, 122001 (2012).

[7] T. K. Pedlar *et al.* (CLEO Collaboration), Phys. Rev. Lett. **107**, 041803 (2011).

[8] C. Z. Yuan *et al.* (Belle Collaboration), Phys. Rev. Lett. **99**, 182004 (2007).

[9] B. Aubert *et al.* (*BABAR* Collaboration), Phys. Rev. Lett. **95**, 142001 (2005).

[10] M. Ablikim *et al.* (BESIII Collaboration), Nucl. Instrum. Methods Phys. Res., Sect. A **614**, 345 (2010).

[11] M. Ablikim *et al.* (BESIII Collaboration), Phys. Rev. Lett. **104**, 132002 (2010).

[12] E. V. Abakumova *et al.*, Nucl. Instrum. Methods Phys. Res., Sect. A **659**, 21 (2011).

[13] M. Ablikim *et al.* (BESIII Collaboration), Phys. Rev. D **86**, 092009 (2012).

[14] J. Beringer *et al.* (Particle Data Group), Phys. Rev. D **86**, 010001 (2012).

[15] A track parameter correction procedure [16] is applied to the MC simulated charged tracks to improve the agreement between the data and MC simulation of the χ^2_{4C} distribution of the kinematic fit. The correction factors are obtained from a high purity control sample $J/\psi \to \phi f_0(980)$, with $\phi \to K^+K^-$ and $f_0(980) \to \pi^+\pi^-$. Reasonable agreement between the data and MC simulation is observed for the channels analyzed in this work. The systematic error of the χ^2_{4C} requirement is taken as half of the correction in the efficiency, which is much larger than the effect due to the uncertainties in the correction factors to cover possible unknown effects in the procedure.

[16] M. Ablikim *et al.* (BESIII Collaboration), Phys. Rev. D **87**, 012002 (2013).

[17] J. P. Lees *et al.* (*BABAR* Collaboration), Phys. Rev. D **86**, 051102(R) (2012).

[18] H. Albrecht *et al.* (ARGUS Collaboration), Phys. Lett. B **241**, 278 (1990).